frontiers in Plant Science

ORIGINAL RESEARCH
published: 05 February 2018
doi: 10.3389/fpls.2018.00067

Decrease in the Photosynthetic Performance of Temperate Grassland Species Does Not Lead to a Decline in the Gross Primary Production of the Ecosystem

*Anthony Digrado[1], Louis G. de la Motte[2], Aurélie Bachy[2], Ahsan Mozaffar[2,3], Niels Schoon[3], Filippo Bussotti[4], Crist Amelynck[3,5], Anne-Catherine Dalcq[6], Marie-Laure Fauconnier[7], Marc Aubinet[2], Bernard Heinesch[2], Patrick du Jardin[1] and Pierre Delaplace[1]**

[1] Plant Biology Laboratory, AGRO-BIO-CHEM, University of Liège-Gembloux Agro-Bio Tech, Gembloux, Belgium, [2] Biosystems Dynamics and Exchanges, TERRA, University of Liège-Gembloux Agro-Bio Tech, Gembloux, Belgium, [3] Royal Belgian Institute for Space Aeronomy, Uccle, Belgium, [4] Department of Agri-Food Production and Environmental Science, University of Florence, Florence, Italy, [5] Department of Analytical Chemistry, Ghent University, Ghent, Belgium, [6] Modelling and Development Unit, AGRO-BIO-CHEM, University of Liège-Gembloux Agro-Bio Tech, Gembloux, Belgium, [7] Agro-Bio Systems Chemistry, TERRA, University of Liège-Gembloux Agro-Bio Tech, Gembloux, Belgium

Edited by:
Rosa M. Rivero,
Centro de Edafología y Biología Aplicada del Segura (CSIC), Spain

Reviewed by:
Lorenzo Ferroni,
University of Ferrara, Italy
Carlos Jose De Ollas,
Jaume I University, Spain
Vicent Arbona,
Jaume I University, Spain

***Correspondence:**
Pierre Delaplace
pierre.delaplace@uliege.be

Specialty section:
This article was submitted to Plant Abiotic Stress, a section of the journal Frontiers in Plant Science

Received: 13 June 2017
Accepted: 12 January 2018
Published: 05 February 2018

Citation:
Digrado A, de la Motte LG, Bachy A, Mozaffar A, Schoon N, Bussotti F, Amelynck C, Dalcq A-C, Fauconnier M-L, Aubinet M, Heinesch B, du Jardin P and Delaplace P (2018) Decrease in the Photosynthetic Performance of Temperate Grassland Species Does Not Lead to a Decline in the Gross Primary Production of the Ecosystem. Front. Plant Sci. 9:67. doi: 10.3389/fpls.2018.00067

Plants, under stressful conditions, can proceed to photosynthetic adjustments in order to acclimatize and alleviate the detrimental impacts on the photosynthetic apparatus. However, it is currently unclear how adjustment of photosynthetic processes under environmental constraints by plants influences CO_2 gas exchange at the ecosystem-scale. Over a 2-year period, photosynthetic performance of a temperate grassland ecosystem was characterized by conducting frequent chlorophyll fluorescence (ChlF) measurements on three primary grassland species (*Lolium perenne* L., *Taraxacum* sp., and *Trifolium repens* L.). Ecosystem photosynthetic performance was estimated from measurements performed on the three dominant grassland species weighed based on their relative abundance. In addition, monitoring CO_2 fluxes was performed by eddy covariance. The highest decrease in photosynthetic performance was detected in summer, when environmental constraints were combined. Dicot species (*Taraxacum* sp. and *T. repens*) presented the strongest capacity to up-regulate PSI and exhibited the highest electron transport efficiency under stressful environmental conditions compared with *L. perenne*. The decline in ecosystem photosynthetic performance did not lead to a reduction in gross primary productivity, likely because increased light energy was available under these conditions. The carbon amounts fixed at light saturation were not influenced by alterations in photosynthetic processes, suggesting photosynthesis was not impaired. Decreased photosynthetic performance was associated with high respiration flux, but both were influenced by temperature. Our study revealed variation in photosynthetic performance of a grassland ecosystem responded to environmental constraints, but alterations in photosynthetic processes appeared to exhibit a negligible influence on ecosystem CO_2 fluxes.

Keywords: carbon fluxes, chlorophyll fluorescence, eddy covariance, grassland, GPP, JIP-test, respiration

INTRODUCTION

Continuous exposure to environmental constraints can negatively affect plant growth and cause yield loss in agricultural crop plants. In particular, environment affects photosynthesis. Photosynthesis and the photosynthetic apparatus can be respectively altered and potentially damaged by elevated air temperatures, high light levels, and drought (Bussotti et al., 2007; Bertolde et al., 2012; Goh et al., 2012; Ashraf and Harris, 2013). Plants, however, can proceed to photosynthetic adjustments in order to acclimatize under stressful conditions and alleviate the detrimental impacts on the photosynthetic apparatus. For instance, under high light, plants promote the dissipation of excess energy within the light harvesting complex to decrease photosystem II (PSII) excitation (Goh et al., 2012; Jahns and Holzwarth, 2012). Plants can also protect PSII by adjusting the electron transport rate within the PSII reaction center (RC) or passing electrons to alternative electron acceptors (Derks et al., 2015). Cyclic electron flow around photosystem I (PSI) can be triggered to alleviate photoinhibition, as it contributes to the generation of an acidic lumen, which promotes energy dissipation via heat through the xanthophyll cycle (Takahashi et al., 2009). Oxidative stress can also result from an imbalance between dark and light-phases of photosynthesis under stressful environmental conditions. In such cases, ATP and NADPH accumulate, but are not converted to ADP and $NADP^+$ to feed the primary reactions (e.g., light phase). Photorespiration, by using ATP and NADPH energy, enables acceptor regeneration for photosynthetic primary reactions and prevents reactive oxygen species (ROS) production (Voss et al., 2013).

Perturbation of photosynthetic processes can impact plant photosynthetic performance, which is defined here as the efficiency in which a photon can be absorbed and used to produce chemical energy. Chlorophyll *a* fluorescence (ChlF) analysis was employed in several studies to investigate the physiological aspects of photosynthesis and characterize plant photosynthetic performance (Murchie and Lawson, 2013; Guidi and Calatayud, 2014). Measure of the fast fluorescent transient (i.e., the OJIP curve) of dark-adapted leaves using a plant efficiency analyser gives information on the "potential" plant photosynthetic performance, whereas a pulse-amplitude modulated fluorimeter provides measures of the actual plant photosynthetic efficiency (Kalaji et al., 2017). Analysis of the OJIP curve derived from a plant efficiency analyser fluorimeter provides useful information related to the photosynthetic apparatus status and functioning (Maxwell and Johnson, 2000). Studies reported ChlF transient analysis using the JIP-test a very useful tool to investigate the photosynthetic apparatus response and adaptive ability to a wide range of stressors (Bussotti et al., 2007, 2010; Redillas et al., 2011; Brestic et al., 2012). Its utilization in ecological studies also demonstrated its relevance in assessing different taxa for photosynthetic properties and characterizing taxon adaptive photosynthetic strategies (Pollastrini et al., 2016a). The JIP-test applies energy fluxes in biomembrane theory to calculate several phenomenological and biophysical parameters that characterize PSII behavior and therefore photosynthetic performance (Strasser et al., 2000). PSI activity was later described using new parameters (Tsimilli-Michael and Strasser, 2008; Smit et al., 2009), which enabled the study of energy fluxes from the plastoquinone pool to the PSI acceptor side. Many studies have contributed to increase the empirical knowledge on the possible association between the shape of the fluorescence transient and the physiological status of the studied sample (Kalaji et al., 2016).

The relationship between the fast fluorescent transient and gas exchange, however, is not straightforward and is still largely debated (Kalaji et al., 2017). While reduced PSII efficiency can be associated with a decreased carbon assimilation (van Heerden et al., 2003; Bertolde et al., 2012), reduction in net photosynthesis are typically related to stomatal limitations (Bollig and Feller, 2014), and/or inactivation of the rubisco enzyme (Feller, 2016). Indeed, a decline in photosynthetic activity can be observed during moderate heat stress without impairment of PSII (Stroch et al., 2010; Pettigrew, 2016) as the entire photosynthetic process is affected at lower temperature than its PSII component alone (Janka et al., 2013). Furthermore, Lee et al. (1999) reported PSII complexes were sometimes observed in excess in leaves and the photosynthetic apparatus is able to suffer considerable damages before a reduction in net photosynthesis occurs. Despite these observations, different photosynthetic responses among species under equal environmental constraints were reported, likely from variable abilities to efficiently use photon energy under stressful conditions (Gravano et al., 2004; Jedmowski et al., 2014; Kataria and Guruprasad, 2015). Differences in photosynthetic component sensitivity to abiotic stress (Oukarroum et al., 2016) also explained varied photosynthetic response to environmental constraints. As a consequence, plants living under different climatic conditions expressed variation in their photosynthetic performance and sensitivity to environmental factors due to local adaptation (Ciccarelli et al., 2016; Pollastrini et al., 2016a,b). This emphasizes the importance to better characterize the photosynthetic functionality of different ecosystems in varied climatic conditions to circumvent climate change impacts on photosynthesis.

Here, we addressed the following questions: (i) do different species and/or taxonomic groups display different response mechanisms; and (ii) do variations in the photosynthetic performance in a grassland ecosystem affect CO_2 fluxes at the ecosystem level. In a previous study, we detected important seasonal variation in the photosynthetic performance of the perennial ryegrass (*Lolium perenne* L.) in a temperate grassland due to the influence of combined environmental constraints (Digrado et al., 2017). However, we did not compare *L. perenne* response to those of other grassland species neither analyse if variations in photosynthetic performance were associated with changes in carbon assimilation by the ecosystem. Indeed, it is likely that grassland species differing in various anatomic aspect (leaf shape, root system…) might express contrasted photosynthetic responses. In such case, it is reasonable to assume that the photosynthetic performance at the ecosystem level must be influenced by its different components (i.e., photosynthetic response at leaf scale for the different species). Based on the current literature, we hypothesize that different species may be characterized by a different photosynthetic performance response explained either by a different acclimatization strategy, stress perception or metabolic response. We also hypothesize that increase in energy dissipation mechanisms at the ecosystem level may be associated with a decrease or a plateau in carbon assimilation as proportionally less photon energy is used for photochemistry. To test our hypothesis, we measured over two growing seasons in field by ChlF the photosynthetic performance response of *L. perenne* and two other important grassland species. ChlF parameters derived from the JIP-test were used to determine which mechanisms triggered the photosynthetic apparatus under stressful environmental conditions and if they differed among species. We also estimated ecosystem level photosynthetic performance by extrapolating leaf-scale measurements and addressed whether an alteration in ecosystem photosynthetic performance affected ecosystem CO_2 fluxes measured using the eddy covariance technique.

MATERIALS AND METHODS

Field Site

The study was conducted within the CROSTVOC project (CROp Stress Volatile Organic Compounds: http://hdl.handle.net/2268/178952) framework. All measurements were performed at the Dorinne Terrestrial Observatory in Belgium (50°18′44′′N 4°58′07′′E). The climate at the site is temperate oceanic. The study area supports permanent grassland, which covers 4.22 ha, and the relief is dominated by a large colluvial depression oriented south-west/north-east. The depression lies on a loamy plateau with a calcareous and/or clay substrate. Altitudes range from 240 m (north-east) to 272 m (south). The paddock was converted to permanent grassland at least 50 years before the start of this study and was intensively grazed by cattle, with the application of cattle slurry and manure. Botanical diversity was evaluated on 24 quadrats (0.5 × 0.5 m) during the months of September 2010 and June 2011. Plant communities were composed of 13 grass species [*Agrostis stolonifera* L., *Alopecurus geniculatus* L., *Bromus hordeaceus* L., *Cynosurus cristatus* L., *Dactylis glomerata* L., *Elymus repens* (L.) Gould, *Festuca pratensis* Huds., *Holcus lanatus* L., *Lolium multiflorum* Lam., *L. perenne*, *Poa annua* L., *Poa pratensis* L., and *Poa trivialis* L.], one N-fixing dicot (*Trifolium repens* L.), and seven non-N-fixing dicots [*Capsella bursa-pastoris* (L.) Medik., *Carduus* sp. L., *Matricaria discoidea* DC., *Plantago major* L., *Ranunculus repens* L., *Stellaria media* (L.) Vill., *Taraxacum* sp.]. The dominant species were *L. perenne*, *Taraxacum* sp. and *T. repens* (Supplementary Table 1).

Micro-Meteorological Data

Grassland micro-meteorological data, including photosynthetic photon flux density (PPFD) (SKP215, Skye Instruments, Llandrindod Wells, UK), air temperature (T_{air}), air relative humidity (RH) (RHT2nl, Delta-T Devices Ltd., Burwell, Cambridge, UK) at 2.62 m above soil level, soil moisture (SM) (CS616, Campbell Scientific Inc., Logan, UT, USA), and soil temperature (T_{soil}) (PT 1000, Campbell Scientific Inc., Logan, UT, USA) at 2 cm depth were recorded every 30 min throughout the measurement period. Vapor pressure deficit (VPD) was calculated from T_{air} and RH measurements.

CO_2 Flux Measurements

CO_2 flux measurements and computation procedures were performed as described by Gourlez de la Motte et al. (2016). High frequency flux losses were corrected following Mamadou et al. (2016). CO_2 flux measurements were conducted using the eddy covariance technique and a three-dimensional sonic anemometer (CSAT3, Campbell Scientific Ltd., UK) coupled with a fast CO_2-H_2O non-dispersive infrared gas analyser (IRGA) (LI-7000, LI-COR Inc., Lincoln, NE, USA) to measure CO_2 fluxes. Air was drawn into the IRGA through a tube (6.4 m long; inner diameter 4 mm) by a pump (NO22 AN18, KNF Neuberger, D) with a 12 l min^{-1} flow at a height of 2.6 m above ground. Data were sampled at a rate of 10 Hz. Zero and span calibrations were performed for CO_2 approximately once per month. Pure nitrogen (Alphagaz 1, Air Liquide, Liege, Belgium) was used for the zero and 350 μmol CO_2 mol^{-1} mixture (Chrystal mixture, Air Liquide, Liege, Belgium) for the span. Net ecosystem CO_2 exchange (NEE) from half-hourly eddy covariance measurements was partitioned into gross primary production (GPP) and total ecosystem respiration (R_{eco}) according to the method described by Reichstein et al. (2005).

The GPP response to PPFD for days where ChlF measurements were performed was fit by a Mitscherlich equation (Dagnelie, 2013) where the quantum light efficiency *a* (i.e., the initial slope of the curve) and $GPP_{\max}$ (i.e., the asymptotic value of GPP for PPFD→ ∞) were deduced using R software version 3.3.0 (R Development Core Team, 2012). Only measurements with PPFD-values above 50 μmol m^{-2} s^{-1} were applied during the procedure. The equation was as follows:

$$GPP\ (PPFD) = GPP_{max} \times \left[1 - exp^{\left(-\frac{\alpha \times PPFD}{GPP_{max}}\right)}\right]$$

This equation was used to calculate GPP_{1500} (i.e., GPP at PPFD = 1,500 μmol m^{-2} s^{-1}) to estimate GPP at light saturation. This parameter was used in this study rather than $GPP_{\max}$ because the latter can lead to GPP overestimation at light saturation. Conclusions of this study were not dependent on this choice, as similar results were obtained applying both parameters.

The response of R_{eco} to T_{soil} for days when ChlF measurements were conducted was fit based on the Lloyd and Taylor (1994) equation where the activation energy E_0 (i.e., respiration sensitivity to temperature) and R_{10} (i.e., dark respiration normalized at 10°C) were deduced from R software version 3.3.0. The equation was as follows:

$$R_{eco}\ (T_{soil}) = R_{10} \times exp\left[E_0 \times \left(\frac{1}{T_{ref}+46.02} - \frac{1}{T_{soil}+46.02}\right)\right]$$

The reference temperature (T_{ref}) was set at 10°C.

Because, respiratory activity is extrapolated from night measurements, CO_2 fluxes estimated at day may have been biased because of several mechanisms related to plant physiology that were not taken into account in this method. The omission of the inhibition of plant mitochondrial respiration by light (Atkin et al., 1997), for instance, may have led to an overestimation of R_{eco} at day (Heskel et al., 2013; Wehr et al., 2016). In contrast, the omission of photorespiratory activity may have led to an underestimation of R_{eco} (Wohlfahrt and Gu, 2015), especially during hot days when photorespiration is high due to the increasing specificity of Rubisco with O_2 at high temperature (Sage, 2013). This have consequences on GPP estimation since it is derived from NEE and R_{eco}. These issues are well known by the eddy covariance researcher community and it is difficult to quantify the contribution of each potential biases in our measurements. By using an adapted "big-leaf photosynthesis model," a study was able to assess the bias in CO_2 fluxes measured by eddy covariance in response to light (Wohlfahrt and Gu, 2015). They showed that R_{eco} was overestimated at low light (ca. <800 μmol m^{-2} s^{-1}) because the mitochondrial inhibition bias overweighed photorespiration in these conditions. In contrast, R_{eco} was underestimated at high light (ca. >800 μmol m^{-2} s^{-1}) because photorespiration became stronger. They also showed that, over a daily cycle, GPP was more representative of the "true photosynthesis" (i.e., gross photosynthesis, carboxylation) rather than the "apparent photosynthesis" (i.e., true photosynthesis minus photorespiration) and only overestimated "true photosynthesis" by 3% on average. This was acknowledged in the interpretations of our results.

Analysis of the Fluorescence Transient Using the JIP Test

Grassland ChlF emission measures were conducted on *L. perenne*, *Taraxacum* sp., and *T. repens* at three plots (each 30 × 5 m) from June to October 2014 and May to October 2015, using a HandyPEA fluorimeter (Hansatech Instruments, Pentney, Norfolk, UK). Cows were allowed to graze between measurement periods. Measurements were performed in each monitored plot 4x day^{-1} at 11:00, 13:00, 15:00, and 17:00 h (local time zone). The number of replicates for each plot and time period was seven in 2014 and eight in 2015. Measurements were performed on non-senescent mature leaves. Prior to each measurement, leaves were dark-adapted with leaf clips for 30 min. The leaf clips applied to *L. perenne* were modified to fit the width of leaves by reducing the measurement surface by half using black vinyl electrical tape, following the manufacturer's recommendations. The dark-acclimated leaf surfaces were then exposed to red light with a flux density of 3,000 μmol m^{-2} s^{-1} for 1 s, which was provided with an array of three light-emitting diodes (peak wavelength at 650 nm). During the 1 s-long excitation with the red light of the sample, the induced fluorescence signal was recorded every 10 μs from 10 to 300 μs, then every 100 μs till 3 ms, then every 1 ms till 30 ms, then every 10 ms till 300 ms, and finally every 100 ms till 1 s.

Fluorescence emissions measured at 50 μs (F_{50}, step O), 300 μs (F_{300}, step K), 2 ms (step J), 30 ms (step I), and maximum (F_{M}, step P) were used to characterize fluorescence emission transients and determine several parameters describing photosynthetic activity based on the JIP test (Strasser et al., 2000, 2004). **Table 1** summarizes the ChlF parameters used in this study. When a ChlF parameter showed an aberrant value (i.e., infinite), all parameters derived from this specific measurement were discarded. This represented <0.16% of the dataset.

Statistical Analyses

Three groups of comparable meteorological conditions were defined by clustering (Ward's method based on the Euclidian distance). Clustering was performed on the coordinates of the two first principal components of a principal component analysis (PCA) (result of the PCA-clustering available in Supplementary Figure 1A). All meteorological parameters (PPFD, T_{air}, VPD, SM, RH, and T_{soil}) were entered as variables in the PCA. The influence of monitored plots on ChlF response was examined using a General Linear Model (GLM) type III. The assigned cluster number previously identified for each time period of measurement were used as a meteorological factor in the GLM analysis. The monitored plots were used in the GLM as a block factor and was considered as random factor. Plot influence was not found significant; therefore ChlF parameter values were averaged for the three species without consideration of the different plots.

Ecosystem photosynthetic performance was approximated from measurements performed on the three dominant grassland species. In order to achieve this, ChlF parameters from the three species were weighed based on the relative abundance of their respective group (i.e., grass, N-fixing dicot, and non-N-fixing dicot) to extrapolate ChlF parameters for the entire pasture/grassland ecosystem. Relative abundance values from the last survey were used (Supplementary Table 1). Three groups of contrasting ecosystem photosynthetic performance based on ecosystem ChlF parameters were then defined using the same methodological approach employed in the meteorological groups (result of the PCA-clustering available in Supplementary Figure 1B). Ecosystem ChlF parameters ($F_{\mathrm{V}}/F_{\mathrm{M}}$, $\mathrm{PI}_{\mathrm{ABS}}$, Ψ_{E0}, and ΔV_{IP}) were entered as variables in this second PCA followed by clustering, with the exception of the raw fluorescence values F_{50} and F_{M} which were used to calculate ChlF parameters. The behavior of the three grassland species within these groups was analyzed. A type III GLM and Tukey's Honest Significant Difference test (Tukey HSD) were used to classify mean ChlF parameter values at species and ecosystem levels, meteorological mean parameter values and CO_2 fluxes among ChlF clusters. Prior to statistical analyses, a correction factor based on the reduction ratio surface measurements of *L. perenne* leaf clips was applied to F_{50} and F_{M}-values to enable the monocot comparisons with those measured on dicot species. ChlF parameters (except for $\mathrm{PI}_{\mathrm{ABS}}$ due to the presence of negative values) and CO_2 fluxes were square root-transformed for type III GLM analyses to improve normality and homogeneity of variances. Photosynthetic processes influence on daily variation in ecosystem respiration and grassland capacity to fix carbon at light saturation were tested by simple linear regressions between the daily amplitude variability in ecosystem ChlF parameters and R_{10} and GPP_{1500}.

Relationships among ChlF-based photosynthetic responses, meteorological conditions, and CO_2 fluxes were explored

TABLE 1 | Summary of parameters and formulas used for the analysis of the fast fluorescence transient OJIP.

Parameters	Equations	Description
TECHNICAL FLUORESCENCE PARAMETERS		
F_t		Fluorescence intensity at the time t.
F_{50}		Fluorescence intensity at 50 μs (O-step).
F_{300}		Fluorescence intensity at 300 μs (K-step).
F_J		Fluorescence intensity at 2 ms (J-step).
F_I		Fluorescence intensity at 30 ms (I-step).
F_M		Maximum fluorescence intensity (P-step).
F_V	$F_m - F_{50}$	Maximum variable fluorescence.
F_V/F_M (= ϕ_{P0})	$1 - (F_{50}/F_M)$	Maximum quantum yield of PSII of a dark adapted leaf. Expresses the probability that an absorbed photon will be trapped by the PSII reaction center.
JIP-TEST DERIVED PARAMETERS		
M_0	$4.[(F_{300} - F_{50}) / (F_M - F_{50})]$	Approximate initial slope of the fluorescence transient.
V_t	$(F_t - F_{50})/(F_M - F_{50})$	Relative variable fluorescence at the time t.
V_J	$(F_J - F_{50}) / (F_M - F_{50})$	Relative variable fluorescence at 2 ms (J-step).
V_I	$(F_I - F_{50}) / (F_M - F_{50})$	Relative variable fluorescence at 30 ms (I-step).
RC/ABS	$\phi_{P0}\ (V_J / M_0)$	Q_A-reducing reaction centers (RC) per PSII antenna Chl.
Ψ_{E0} (= J phase)	$1 - V_J$	The efficiency with which a photon trapped by the PSII RC moves an electron into the electron transport chain beyond Q_A.
ΔV_{IP} (= I–P phase)	$1 - V_I$	The efficiency with which a photon trapped by the PSII RC moves an electron into the electron transport chain beyond PSI to reduce the final acceptors of the electron transport chain, i.e., ferredoxin and NADP$^+$.
PI_{ABS}	$(RC/ABS)\ [\phi_{P0} / (1 - \phi_{P0})]\ [\Psi_{E0} / (1 - \Psi_{E0})]$	Performance index (potential) on absorption basis for energy conservation from photons absorbed by PSII to the reduction of intersystem electron acceptors.

The nomenclature used is in agreement with the work of Strasser et al. (2000, 2004).

using Canonical Correlation Analysis (CCA). This multivariate statistical test serves to identify linear combinations among random variables between two datasets (e.g., ChlF and meteorological data) in order to maximize their correlation. The two new sets of canonical variates, constructed based on the original datasets, determine a pair of canonical variates with a maximized simple correlation. Each set of constructed canonical variates has a variance = 1 and are uncorrelated with other constructed variates. The correlation relevance between the two groups of datasets is tested by the significance of the correlation between the pairs of canonical variates. Significance in at least one canonical pair means the two analyzed datasets are not independent and enable the associations among the different variables. Compared with the Pearson correlation test, CCA explores interdependence within a set of variables. Approach of the canonical correlation is very similar to PCA as axis are a linear combination of data. However, in contrast to PCA where linear combination maximizes the variance on the first axis, CCA maximizes the correlation between two datasets. Three CCA analysis were performed by combining ChlF and meteorological data; meteorological and CO_2 fluxes data; and ChlF and CO_2 fluxes data. An alternative representation of the relationship between ChlF response and meteorological conditions is available in Supplementary Material where clusters of contrasted meteorological condition were represented along clusters of contrasted ecosystem photosynthetic performance in the PCA environment computed based on ChlF data (Supplementary Figure 1C).

All analyses were performed using the software Minitab® version 17.1.0 (State College, Pennsylvania, USA) and R software version 3.3.0 with the following R package: "FactoMineR" (Husson et al., 2016), "Vegan" (Oksanen et al., 2012), "CCP" (Menzel, 2015), "Car" (Fox et al., 2016), and "Relaimpo" (Groemping and Matthias, 2013).

RESULTS

Environmental Conditions

The highest solar irradiance values were detected during summer (i.e., May to August) for both years, with midday PPFD-values above 1,500 μmol m^{-2} s^{-1} (**Figure 1A**). This period was also characterized by the highest midday T_{air} and VPD-values, which exceeded 30°C and 2.0 kPa, respectively (**Figures 1B,D**). Autumn (i.e., September to October) was characterized by PPFD, T_{air}, and VPD-values below 1,500 μmol m^{-2} s^{-1}, 25°C, and 1 kPa, respectively, for most ChlF measurement days. Three specific meteorological events were observed in the grassland during the second year of the study. A heat wave from 30 June to 5 July 2015 (**Figure 1A**) characterized by six consecutive days with maximum T_{air} between 28.9 and 34°C, and two dry spells with ∼20% SM during the months of June and July 2015 (**Figure 1C**).

Grassland ChlF Parameters Evolution and Influence of Environmental Conditions

Grassland ChlF parameters exhibited diurnal variation and showed a pattern consistent with PPFD (**Figures 1A, 2**). Indeed, while other environmental parameters such as T_{air} and VDP were still high at the end of the day, ChlF parameters usually went back to a value similar to that of the first measurement

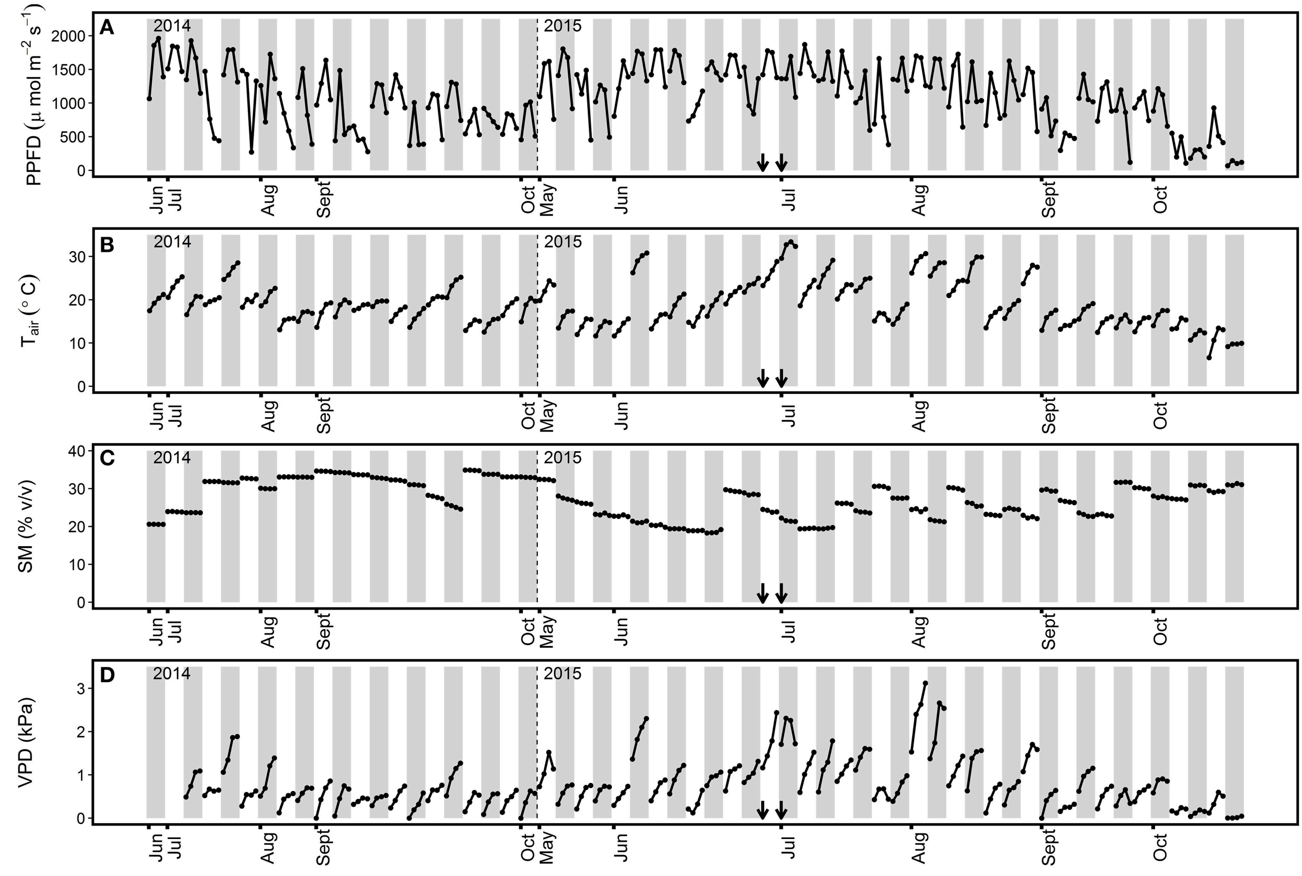

FIGURE 1 | Environmental conditions encountered during chlorophyll fluorescence measurements in the 2014 and 2015 study periods. Values at 11, 13, 15, and 17 h for each day of chlorophyll fluorescence measurements are represented for **(A)** PPFD, photosynthetic photon flux density; **(B)** T_{air}, air temperature; **(C)** SM, soil moisture at a depth of 5 cm; **(D)** VPD, vapor pressure deficit. Gray bars separate the different days of measurements. The arrows indicate the first and third day of the heat wave. Modified from Digrado et al. (2017).

performed, following the diurnal pattern of PPFD. Variation in ChlF parameters for the three grassland species was highest in summer, where the greatest diurnal increases/decreases were measured around midday, when high PPFD-values were measured with high T_{air} and VPD. During the midday period, frequent declines in absorbed photon energy use efficiency, expressed as a strong decrease in maximum quantum yield of primary photochemistry (F_V/F_M) and performance index (PI_{ABS}) were observed for the three grassland species. These declines were characterized by decreased F_V/F_M- and PI_{ABS}-values as low as 0.12 and < 0.01, respectively. In contrast, a stable F_V/F_M-value of ~0.76 was measured in autumn for the three grassland species, indicating high PSII performance during this period. During the summer sampling period, observed midday decreases in F_V/F_M were accompanied by increases in the efficiency to reduce the end electron acceptor (ΔV_{IP}) for the three measured grassland species (**Figure 2E**). More stable ΔV_{IP}-values of ~0.31 were observed in autumn. Reduced variation in electron transport efficiency beyond Q_A (Ψ_{E0}) (**Figure 2B**) was observed, with stable values of ~0.53 for Ψ_{E0}. Changes in Ψ_{E0} were only observed during episodes with high increased ΔV_{IP}. During these episodes, the three grassland species presented the following contrasting Ψ_{E0} response: strong augmentation in Ψ_{E0} were observed in *Taraxacum* sp. and *T. repens*, whereas *L. perenne* showed reduced variation or even decreased Ψ_{E0}.

Three groups of contrasted ecosystem photosynthetic performance were determined by PCA-clustering (**Table 2**). The first group (C1) was characterized by a high capacity to employ photon energy, illustrated by high F_V/F_M- and PI_{ABS}-values for the ecosystem and the three grassland species. C1 cluster response was characterized as dominant in autumn and was detected in 171 observed time periods (**Figure 2A**). *L. perenne* and *Taraxacum* sp. exhibited the highest PI_{ABS} values in the C1 group. In contrast, the third group (C3) was characterized by the lowest F_V/F_M and PI_{ABS}-values for the grassland ecosystem and the three species, demonstrating low photosynthetic performance. The photosynthetic response characterized by this group was detected in 11 observed time periods and the responses were only detected in summer, particularly at midday (**Figure 2A**). *Taraxacum* sp. presented the highest F_V/F_M-values in this group, whereas the lowest values were observed in *T. repens*. The second group (C2) showed intermediate F_V/F_M- and PI_{ABS}-values, where *Taraxacum* sp. exhibited the highest

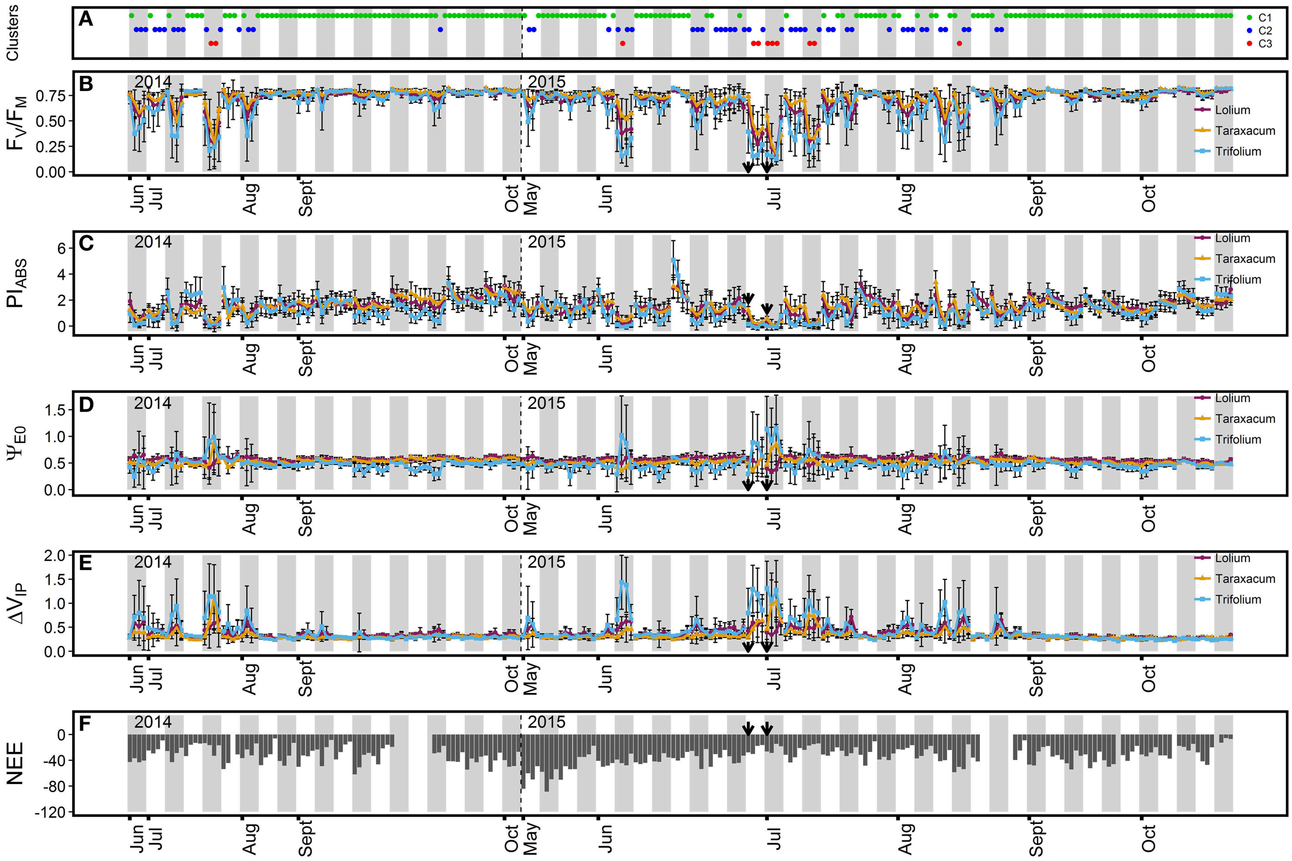

FIGURE 2 | Time course of ChlF parameters (**B**, F_V/F_M; **C**, PI_{ABS}, **D**, Ψ_{E0}; and **E**, ΔV_{IP}) for the three grassland species and net ecosystem CO_2 exchange (**F,** NEE, μmol CO_2 m^{-2} s^{-1}) during the two measurement campaign in the grassland. For each measured day, the ChlF parameter average value ($n = 21$ or 24) ± SD for each of the four measurement time periods (11:00, 13:00, 15:00, and 17:00 h) is represented for the three grassland species (purple, *L. perenne*; orange, *Taraxacum* sp.; light blue, *T. repens*). **(A)** ChlF cluster (green, C1; dark blue, C2; red, C3) the group has been assigned during each time period by the Principal Component Analysis (PCA)-clustering. Gray bars separate the different days of measurements. The arrows indicate the first and third day of a heat wave. A focus on ChlF parameters and NEE variations during the heat wave period is available in Supplementary Figure 2.

F_V/F_M-values in C2. Photosynthetic response characterized by this cluster was observed throughout the season in 54 observed time periods (**Figure 2A**). These results indicated that the grassland ecosystem was more efficient in photon energy use for photochemistry in autumn. Increased initial fluorescence (F_{50}) and decreased maximum fluorescence yield (F_M) were responsible for decreased F_V/F_M-in clusters C2 and C3 (**Table 2**). Only moderate Ψ_{E0} changes were observed in the three species between the C1 and C2 clusters. However, results indicated differences in electron transport efficiency between dicot and monocot species beyond Q_A in the C3 cluster. Indeed, dicot species exhibited either a stable (non-significant Ψ_{E0} increase for *Taraxacum* sp. even though high values were recorded in July 2014 and July 2015) or an increased value (+86% Ψ_{E0} increase for *T. repens*) of Ψ_{E0} whereas a decrease in Ψ_{E0} was observed for *L. perenne* (−19%). F_V/F_M-and PI_{ABS}-decreased values were accompanied by increases in ΔV_{IP} for dicot species in clusters C2 and C3. *L. perenne*, however, did not exhibit a significant change in ΔV_{IP} between the cluster C2 and C3 despite changes in environmental conditions (**Table 2**). The photosynthetic ecosystem response based on ChlF parameters was similar to *L. perenne* as the contribution of grass species to the ecosystem response was estimated at 88.6%.

CCA analysis revealed significant correlations between environmental factors and the photosynthetic performance of the studied grassland species and the ecosystem; correlation for the first and the second canonical pairs equalled to 88.6% ($P < 0.001$) and 60.5% ($P < 0.001$) respectively (**Figure 3A**). ChlF parameters F_V/F_M, PI_{ABS}, and ΔV_{IP} showed similar relationships with environmental parameters for the three species. Decreased F_V/F_M and PI_{ABS} was associated with increased PPFD, VPD, T_{air}, and T_{soil}, and decreased RH and SM. These results suggested a decline in photosynthetic performance under these conditions, typically observed in summer, especially at midday. Compared with F_V/F_M and PI_{ABS}, ΔV_{IP} exhibited an opposite relationship with environmental parameters. The parameter representative of electron transport efficiency beyond Q_A, Ψ_{E0}, was least influenced by meteorological parameters, particularly for *L. perenne*. SM exhibited the lowest influence on ChlF parameters. ChlF parameters which described the ecosystem

TABLE 2 | Description of the three clusters of photosynthetic performance (PP) based on ChlF measurements (C1, C2, and C3) for each grassland species and the ecosystem, and the prevailing micrometeorological conditions.

			Average in the Different Clusters and Associated Relative Change				
			C1	**C2**	**Δ%**	**C3**	**Δ%**
Species PP	Lolium	F_V/F_M	0.755^{A}	0.610^{C}	−19	0.322^{F}	−57
		PI_{ABS}	1.807^{A}	0.894^{C}	−51	0.150^{D}	−92
		Ψ_{E0}	0.565^{C}	0.608^{B}	+8	0.458^{EF}	−19
		ΔV_{IP}	0.324^{E}	0.516^{C}	+59	0.497^{C}	+54
		F_{50}	459^{F}	558^{D}	+21	791^{B}	+72
		F_M	1895^{B}	1530^{D}	−19	1192^{E}	−37
	Taraxacum	F_V/F_M	0.768^{A}	0.662^{B}	−14	0.398^{E}	−48
		PI_{ABS}	1.736^{AB}	1.052^{C}	−39	0.269^{D}	−85
		Ψ_{E0}	0.531^{D}	0.520^{DE}	−2	0.568^{BCD}	+7
		ΔV_{IP}	0.294^{F}	0.384^{D}	+31	0.687^{B}	+134
		F_{50}	519^{E}	607^{C}	+17	856^{B}	+65
		F_M	2262^{A}	1940^{B}	−14	1517^{D}	−33
	Trifolium	F_V/F_M	0.746^{A}	0.503^{D}	−33	0.206^{G}	−72
		PI_{ABS}	1.592^{B}	0.541^{D}	−66	0.072^{D}	−95
		Ψ_{E0}	0.470^{F}	0.472^{F}	0	0.618^{A}	+89
		ΔV_{IP}	0.312^{EF}	0.618^{B}	+98	1.139^{A}	+264
		F_{50}	566^{D}	821^{B}	+45	1178^{A}	+108
		F_M	2277^{A}	1805^{C}	−21	1500^{D}	−34
Ecosystem PP		F_V/F_M	0.755^{A}	0.607^{B}	−20	0.320^{C}	−58
		PI_{ABS}	1.791^{A}	0.884^{B}	−51	0.153^{C}	−91
		Ψ_{E0}	0.558^{B}	0.595^{A}	+7	0.489^{C}	−12
		ΔV_{IP}	0.322^{B}	0.514^{A}	+60	0.544^{A}	+62
		F_{50}	469^{C}	575^{B}	+23	816^{A}	+74
		F_M	1938^{A}	1568^{B}	−19	1228^{C}	−37
Meteorological conditions		PPFD	917^{B}	1463^{A}	+59	1639^{A}	+79
		T_{air}	17.06^{C}	23.84^{B}	+40	28.27^{A}	+66
		VPD	0.59^{B}	1.34^{A}	+129	1.67^{A}	+185
		SM	28.37^{A}	25.07^{B}	−12	23.86^{B}	−16
		RH	72.57^{A}	57.22^{B}	−21	57.29^{B}	−21
		T_{soil}	14.69^{B}	18.71^{A}	+27	20.21^{A}	+38

Mean values are represented for each cluster. The relative change (Δ%) in the mean with respect to cluster 1 is indicated for clusters 2 and 3. PPFD, photosynthetic photon flux density (μmol m^{-2} s^{-1}); T_{air}, air temperature (°C); VPD, vapour pressure deficit (kPa); SM, soil moisture at a depth of 5 cm (% v/v); RH, relative air humidity (%); T_{soil}, temperature of soil at a depth of 2 cm (°C). Different letters indicate significant differences among the clusters (Tukey HSD, $\alpha = 0.05$) within species, ecosystem, or micrometeorological data.

photosynthetic performance exhibited a similar relationship with meteorological parameters than ChlF parameters describing *L. perenne* response.

Influence of Environmental Conditions and ChlF-Based Photosynthetic Parameters on Co$_2$ Fluxes

Significant correlations between environmental factors and CO$_2$ fluxes, with correlations for the first and the second canonical pairs equal to 78.8% ($P < 0.001$) and 54.7% ($P < 0.001$) respectively, were shown by the CCA (**Figure 3B**). Elevated R_{eco} and GPP fluxes were associated with high PPFD, T_{air}, T_{soil}, and VPD, but low RH- and SM-values. R_{eco} was primarily correlated with temperature and VPD, whereas GPP was mainly correlated with PPFD, suggesting an augmentation of photosynthetic activity with increased light energy availability.

The same approach was used to determine the influence of ecosystem photosynthetic performance on CO$_2$ fluxes (**Figure 3C**). The correlation for the first canonical pair was 72.4% ($P < 0.001$) while the correlation for the second canonical pair was not significant ($P = 0.155$). The relationship between ChlF parameters and CO$_2$ fluxes was therefore defined by the correlation of variables on the first canonical pair. High CO$_2$ flux values were associated with high ΔV_{IP}-values and low F_V/F_M- and PI$_{ABS}$-values. This was particularly noted in R_{eco}, where GPP was mainly represented on the second canonical axis and poorly correlated with ChlF parameter variation. The ChlF parameter Ψ_{E0} was least related with CO$_2$ flux changes, as it was poorly represented on the first canonical axis.

Linear regression detected the absence of significant relationships between variation in ChlF parameters with GPP$_{1500}$ and R_{10} (**Figure 4**), suggesting the influence of changes in photosynthetic processes was negligible. Average

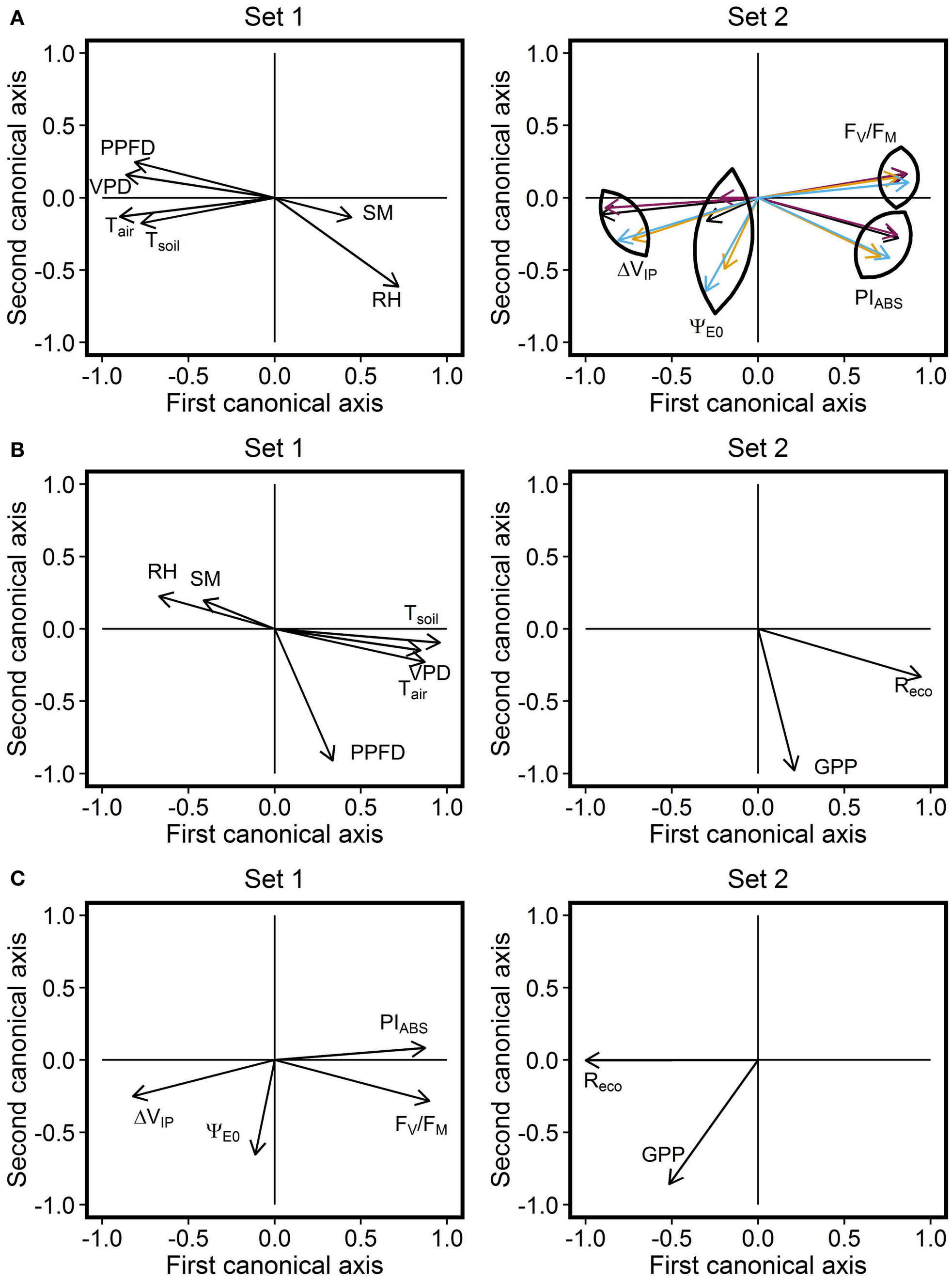

FIGURE 3 | Correlation circle derived from the Canonical Correlation Analysis (CCA). CCA was performed by combining the **(A)** meteorological parameters and ChlF parameters (with distinction between purple, *L. perenne*; orange, *Taraxacum* sp.; blue, *T. repens*; black, ecosystem) data. This analysis establishes a multivariate relationship between parameters from the two datasets. Correlations between the first canonical axis of the two CCA plots and between the second canonical axis of the two CCA plots were 88.6% [Wilks' Lambda = 0.071, $F_{(96,1,173)} = 7.26$, $P < 0.001$] and 60.5% [Wilks' Lambda = 0.333, $F_{(75,\ 995)} = 3.42$, $P < 0.001$], respectively. The same approach was then used by combining **(B)** meteorological parameters and CO_2 flux data. Correlations between the first canonical axis of the two CCA plots and between the second canonical axis of the two CCA plots were 78.8% [Wilks' Lambda = 0.266, $F_{(12,\ 402)} = 31.44$, $P < 0.001$] and 54.7% [Wilks' Lambda = 0.701, $F_{(5,\ 202)} = 17.26$, $P < 0.001$], respectively. Finally, the same approach was used by combining **(C)** ecosystem ChlF parameters and CO_2 flux data. Correlations between the first canonical axis of the two CCA plot and between the second canonical axis of the two CCA plots were 72.4% [Wilks' Lambda = 0.468, $F_{(8,\ 422)} = 24.4$, $P < 0.001$] and 15.6% [Wilks' Lambda = 0.976, $F_{(3,\ 212)} = 1.8$, $P = 0.155$], respectively. PPFD, photosynthetic photon flux density (μmol m^{-2} s^{-1}); T_{air}, air temperature (°C); VPD, vapor pressure deficit (kPa); SM, soil moisture at a depth of 5 cm (% v/v); RH, relative air humidity (%); T_{soil}, temperature of soil at a depth of 2 cm (°C); R_{eco}, respiration of the ecosystem (μmol CO_2 m^{-2} s^{-1}); GPP, gross primary productivity (μmol CO_2 m^{-2} s^{-1}).

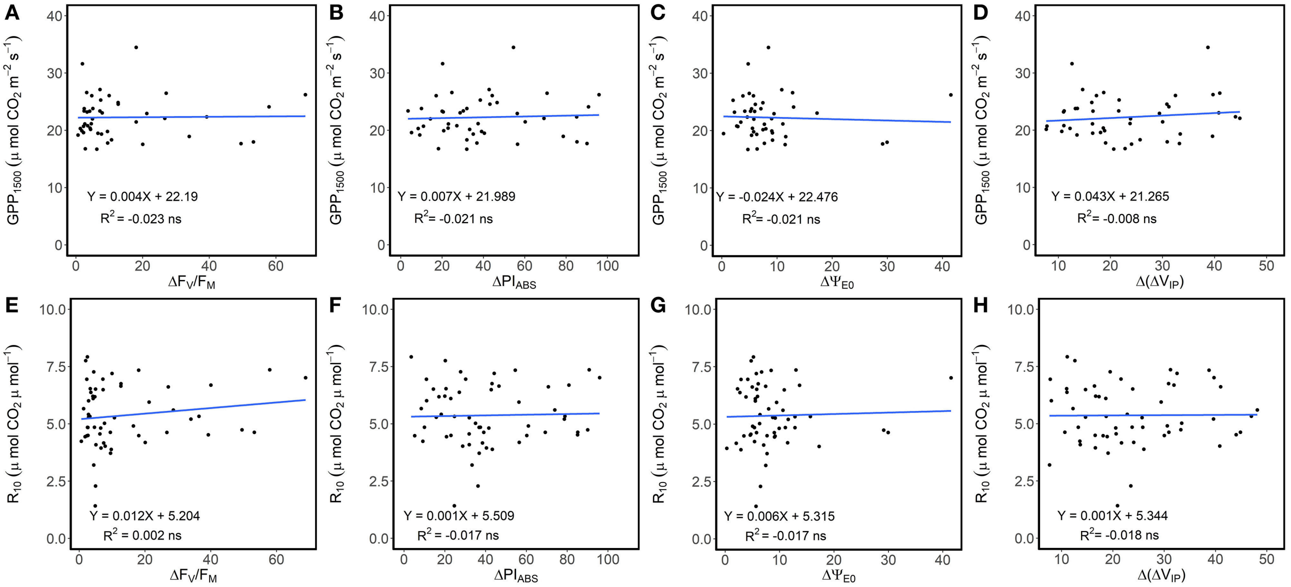

FIGURE 4 | Linear regression between **(A–D)** gross primary productivity at light saturation (GPP_{1500}) and the daily variation of ecosystem ChlF parameters (F_V/F_M, PI_{ABS}, Ψ_{E0} and ΔV_{IP}) and **(E–H)** dark respiration normalized at 10 °C (R_{10}) and the daily variation of ecosystem ChlF parameters. Data were not root squared transformed for this test, but relationships were similar on transformed data and results are not dependent of this choice.

NEE decreased in absolute value with decreased ecosystem photosynthetic performance (**Figure 5A**). However, reduction in net CO_2 uptake by the grassland was not significant. Ecosystem respiration exhibited an opposite trend and increased with decreased ecosystem photosynthetic performance (**Figure 5D**), probably due to its strong correlation with temperature (**Figure 3B**). Stable R_{10}-values detected in the three photosynthetic performance clusters (**Figure 5E**) supported this hypothesis. The lowest GPP values were observed during periods of high photosynthetic performance, while the highest GPP values were observed at lower ecosystem photosynthetic performance (i.e., C2 and C3 clusters) (**Figure 5B**). Difference in GPP between the C2 and C3 ChlF clusters was not significant, despite reduced potential performance of photosynthesis in the C3 cluster. The three photosynthetic performance clusters showed the absence of differences in GPP_{1500}-values (**Figure 5C**), indicating GPP_{1500} was not affected by ecosystem photosynthetic performance.

DISCUSSION

Combined Abiotic Stresses in Summer Led to a Decline in PSII Photosynthetic Performance

The three grassland species examined showed strong decreases in photosynthetic performance in summer (**Figure 2**), when environmental constraints were combined (**Figure 1**). Important F_V/F_M decreases in summer were reported in various ecosystems (Fernández-Baco et al., 1998; Bussotti, 2004; Ciccarelli et al., 2016) and primarily attributed to an excess in solar radiation. A relationship between F_V/F_M and PPFD was confirmed in our study by a similar diurnal evolution and strong correlation between the parameters (**Figure 3A**). Werner et al. (2001, 2002) interpreted the reduction in PSII photochemical efficiency as a protective mechanism, serving to preserve PSII by dissipating excess light energy as heat. The associated increase in F_{50} also suggests the dissociation of the antenna complex from the PSII which might contribute to the reduction of the transfer of excess energy to the RC (Mathur and Jajoo, 2015). Such reorganization within the thylakoid membrane has been observed in *Arabidopsis thaliana* (ecotype Col-0) after long-term acclimatization to high light and was characterized by the detachment of the moderately bound LHCII trimer from the PSII supercomplexes (Bielczynski et al., 2016). It is also possible that a (zeaxanthin-antheraxanthin)-dependent sustained non-photochemical quenching was operating during sunny days and contributed to the reduction of F_V/F_M. In such situation, some components of the non-photochemical quenching can still operate after dark-adaptation and lead to the measurement of not fully unquenched F_M-values (i.e., not fully relaxed in darkness) (Adams and Demmig-Adams, 2004). However, such sustained energy dissipation mechanism is usually observed at low temperature while warm condition (such as observed at midday) was observed to efficiently relax this photoprotection process (Demmig-Adams and Adams, 2006).

High temperature can also lead to reversible conformational changes in some RC, which can no longer reduce Q_A. These "silent RC" act as excitation energy traps, where the energy is subsequently dissipated (Bussotti, 2004; Strasser et al., 2004). This reduction in the PSII donor side efficiency can lead to

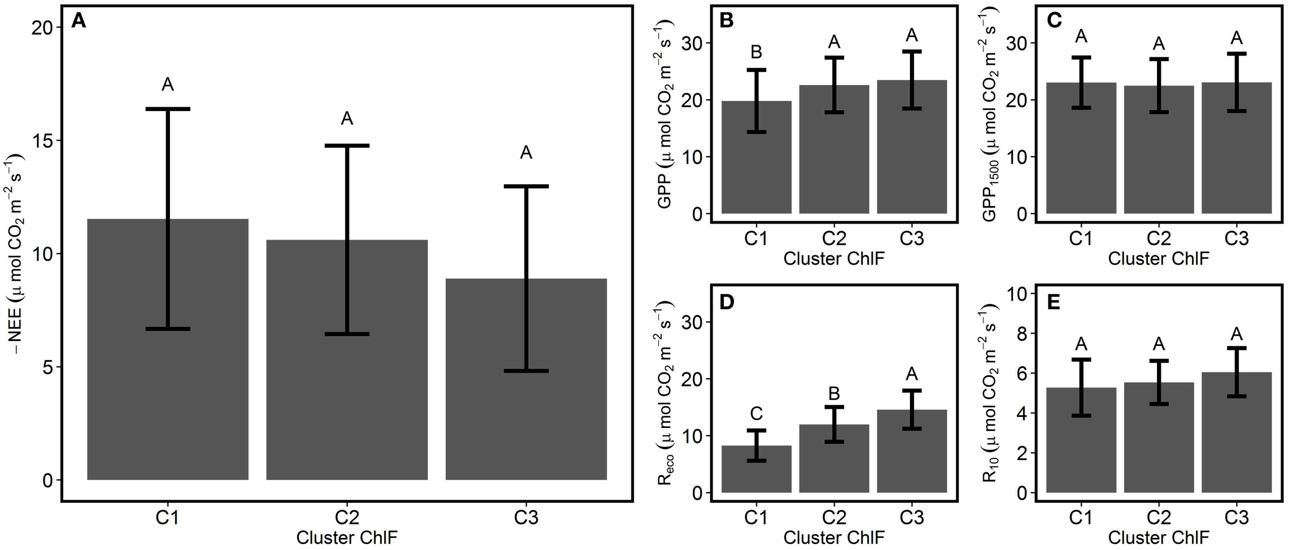

FIGURE 5 | Average CO_2 fluxes associated with the different ecosystem photosynthetic performance clusters. The average ± SD **(A)** NEE, net ecosystem CO_2 exchange; **(B)** GPP, gross primary productivity; **(C)** GPP_{1500}, GPP at light saturation **(D)** R_{eco}, respiration of the ecosystem; and **(E)** R_{10}, dark respiration normalized at 10°C were compared for the different photosynthetic performance responses based on the ChlF clusters defined during the PCA-clustering analysis. Different letters indicate significant differences among the clusters (Tukey HSD, α = 0.05).

decreased F_M (Mathur et al., 2011), which was observed in our study (**Table 2**). RC inactivation also caused F_V/F_M and RC/ABS reductions (data not shown), which exhibited strong diurnal decreases and were responsible for the low midday PI_{ABS} values in summer during hot sunny days (**Figure 2C**). End of day increased PI_{ABS} along with reduced PPFD indicated PSII functionality was not irreversibly impaired, but rather down-regulated. PI_{ABS} reductions reaching 95% in the C3 cluster for the three grassland species (**Table 2**) suggest a high capacity to dissipate excess excitation energy within PSII under stressful environmental conditions.

The PSII is generally described as drought-resistant (Kalaji et al., 2016) although drought-induced damages to the PSII are observed in situation of severe drought stress (Goltsev et al., 2012) especially in sensitive variety (Ghotbi-Ravandi et al., 2014). It is difficult to assess the potential impact of the two dry spells periods observed in June and July 2015 on ChlF parameters because of the low amount of data and the implication of other environmental factors during this period, especially in July due to the heat wave. Regarding the June period, most of the ChlF measurements performed during this period belonged to the high photosynthetic performance cluster, which suggests a low/negligible impact of the relatively low soil moisture content on ChlF parameters. This is in accordance with the low influence of soil moisture observed on ChlF parameters (**Figure 3A**). This does not exclude, however, the influence of soil moisture in combination with other environmental factors as low soil moisture was suggested to enhance PSII sensitivity to heat stress in cottonwood (Tozzi et al., 2013) and *L. perenne* at this site (Digrado et al., 2017).

Studied Dicot Species Exhibited the Highest Capacity to Increase PSI Efficiency

High midday ΔV_{IP}-values measured in summer (**Figure 2E**) suggested up-regulation of the photochemical pathway for de-excitation under stressful conditions (Pollastrini et al., 2011; Desotgiu et al., 2012a), particularly in dicot species (**Table 2**). Cascio et al. (2010) suggested rapid reduction of the end electron acceptor might play a role in protecting the photosynthetic structure by limiting the accumulation of unmanaged electrons beyond the PSI acceptor side, which contributes to the formation of ROS in sunny environments. Increased PSI efficiency was accompanied by increased electron flux efficiency beyond Q_A in the C3 cluster for dicots, especially in *T. repens* (**Table 2**). It is possible that electron flow in the electron transport chain was stimulated by increased PSI efficiency. Interestingly, these changes in ΔV_{IP} and Ψ_{E0} in the C3 cluster were more related to an increase in air temperature than in light availability (**Table 2**) emphasizing the influence of temperature in these processes. This might suggests that PSI accepted almost all electrons as electron supply by the PSII was partly inhibited by high temperature (Brestic et al., 2012).

In contrast, *L. perenne* did not exhibit increased electron transport efficiency beyond PSI between the C2 and C3 clusters and a decrease in Ψ_{E0} was observed (**Table 2**). This limitation in PSI efficiency could be attributed to PSI photoinhibition due to light-induced oxidation of the PSI iron-sulfur component commonly observed in condition of chilling temperature (Scheller and Haldrup, 2005). It was also shown in a recent study that such inactivation of PSI can be observed at high light and at room temperature (Tiwari et al., 2016). Inactivation of the PSI induced by light, however, would require a flux of electrons from the PSII higher than the PSI acceptor side could handle. Therefore, photoinhibition of PSI could be questioned in our case as a decrease in the efficiency of electron transport beyond Q_A was also observed. The decrease in Ψ_{E0} observed in our study can be interpreted as a mechanism to preserve PSI under imbalance between electrons leaving PSII and those reaching electron acceptors beyond PSI (Cascio et al., 2010; Bussotti et al., 2011). A high electron flux under sunny environments might lead to the formation of "free electrons" if the availability of end electron acceptors is insufficient. The free electrons can subsequently activate oxygen and lead to hydrogen peroxide production (Asada, 2006). Reduction in electron transport efficiency beyond Q_A might therefore contribute to the reduction of "free electron" accumulation, and therefore, oxidative damage. Further experimentations such as the measurements of the actual electron flow through leaf gas exchange measurements and the monitoring of PSI RC oxidation by leaf transmission changes at the 820 nm wavelength band would be required to test and verify these hypotheses.

Decline in Photosynthetic Performance Did Not Lead to a Decrease in GPP

GPP variation was well-explained by environmental conditions, such as PPFD, compared with ecosystem photosynthetic performance (**Figure 3**). Moreover, declined ecosystem photosynthetic performance did not result in reduced carbon uptakes (**Figure 5B**). The absence of GPP decrease during episodes of high-energy dissipation can be explained by increased photons received during these periods. Stable GPP-values in C2 and C3 clusters (**Figure 5B**) also suggested the lack of stomatal limitations to carbon assimilation in the grassland during summer stress conditions.

The carbon amounts fixed by the ecosystem at light saturation were not affected by the ecosystem photosynthetic performance (**Figure 5C**) or variation in the different photosynthetic processes (**Figure 4A**). A close relationship between F_V/F_M and carbon uptake was found in studies on maize plants and fodder shrubs, particularly under severe stress, when non-stomatal components effected photosynthesis (Xu et al., 2008; Boughalleb et al., 2009). Our results suggested the absence of non-stomatal limitations in photosynthesis and high ecosystem tolerance to environmental stress during the study but for a particular period of time in which high VPD and T_{air} were recorded.

A previous study conducted at the Dorinne Terrestrial Observatory has shown that herbage height was subjected to small variation during the grazing season as the stocking density was adapted to plants (re)growth by the farmer (Gourlez de la Motte et al., 2016). Beginning of the grazing season in May 2015, however, was characterized by a higher herbage height which might have been responsible for the higher GPP and the stronger negative NEE fluxes observed at this period (**Figure 2F**) as higher biomass has been associated to higher negative NEE in another grazed temperate grassland study (Zhu et al., 2015). Outside this period, we do not expect a significant influence of variation in biomass on CO_2 fluxes as herbage height only fluctuated by around 2 cm (data not shown).

Photosynthesis Saturation Was Associated with PSI Limitations to Manage High Electron Flux

Results indicated a lack of GPP increase between C2 and C3 clusters despite increasing temperature, suggesting optimal temperature conditions and/or photosynthetic saturation due to high PPFD recorded under these conditions. Subsequently, an associated absence of significant increased ΔV_{IP} was observed for the ecosystem whereas dicot species exhibited a significant ΔV_{IP} increase in these conditions (**Table 2**). The incapacity for additional carbon assimilation by the grassland ecosystem under these conditions might be attributed to an impairment of the PSI acceptor side to manage a higher electron flux. Indeed, a high correlation between net photosynthesis and I-P phase related parameters was found in ozone stress studies under high light (Cascio et al., 2010; Desotgiu et al., 2012b), suggesting this OJIP curve region might be applied as a probe for the photosystem's capacity to feed the Calvin-Benson cycle. In our study, however, we detected a weak correlation ($r = 0.111$, $P < 0.001$, data not shown) between the I-P phase and photosynthetic activity (i.e., GPP) compared with r-values reported in the aforementioned studies ($r = 0.324$ and 0.425 for Cascio et al., 2010 and Desotgiu et al., 2012b, respectively). The lower coefficient we observed might be explained because gas-exchanges were not measured on specific leaf species, but resulted from a blend of different species.

It is also likely that photorespiration activity in the grassland have increased with increasing temperature (Sage, 2013), competing with Rubisco carboxylation and thus reducing the apparent photosynthesis (i.e., "true photosynthesis" minus photorespiration). Photorespiration serves a protective role in the photosynthetic apparatus, particularly under excess light conditions, by consuming excess photon energy and preserving PSII from photodamage (Bai et al., 2008; Massacci et al., 2008). Increased photorespiration can stimulate the apparent linear electron transport, which is not fully dedicated to carbon fixation (Rho et al., 2012; Osório et al., 2013). Increase in the efficiency of electron transport beyond PSI and Q_A was measured in dicot species in the absence of GPP increase in the C3 cluster and can be indicative of an increase in photorespiration activity. Dicot species, however, only represented 11.4% of the population, which questions dicots contribution to CO_2 fluxes. In addition, as explained in the material and methods section, GPP in high light condition is likely to more representative of "true photosynthesis," which represents only carboxylation activity and would not reflect increase in Rubisco oxygenation. It is also possible that the observed increase in the electron transport efficiency for dicots results from enhanced cyclic electron transport, a mechanism involved in the protection of the photosynthetic apparatus under high light (Takahashi et al., 2009; Kalaji et al., 2012). This hypothesis is supported by the associated ΔV_{IP} increase which was also observed by Campos et al. (2014) in *Agave salmiana* Otto ex Salm-Dyck seedlings where the enhancement in cyclic electron flow had promoted PSI activity.

High Respiration Activity Was Associated with Low Photosynthetic Performance

Total ecosystem respiration increased with temperature in the grassland (**Figure 3B**), most likely due to increased enzyme activity. Aboveground vegetation and soil might have contributed to increased R_{eco}. Indeed, several studies demonstrated that soil respiration (i.e., root and microbial components) responded positively to increasing temperature (Borchard et al., 2015; Hill et al., 2015; Chen et al., 2017). Belowground respiration might have been an important contributor to R_{eco}, as soil respiration represented more than 70% of ecosystem respiration in an alpine grassland study (Ganjurjav et al., 2014). However, Hoover et al. (2016) cautions comparisons of CO_2 soil fluxes among studies must be conducted carefully, as different plant communities were shown to influence soil respiration. The potential important soil respiration contribution to R_{eco} increase, however, does not exclude the potentially for increased vegetation respiration. Atkin and Tjoelker (2003) reported plant respiration responded positively to increasing temperature. Chen et al. (2016) also showed the response of carbon flux to warming was dependent on plant functional types in meadow grasslands, emphasizing the integral role of vegetation on aboveground fluxes. Our results did not determine the contribution of aboveground vegetation and soil to R_{eco} fluxes.

Increasing ecosystem respiration was also associated with decreasing photosynthetic performance (**Figures 3C**, **5D**). This observation, however, might result from the common R_{eco} and photosynthetic processes sensitivity to temperature, as decreased photosynthetic performance was associated with increased temperature (**Figure 3A**). Moreover, the absence of a significant linear relationship between variation in ChlF parameters and R_{10} (**Figure 4**) suggested the R_{eco} response to temperature was not influenced by changes in photosynthetic processes measured by ChlF. Because photorespiratory activity was not taken into account in the partitioning, R_{eco} may have been underestimated, especially during hot and sunny days. Even though the absence of significant increase in the efficiency of electron transport beyond PSI and Q_A for the ecosystem suggests a negligible activity of alternative electron sink, this hypothesis need to be confirmed by gas-exchange measurements at leaf scale.

CONCLUSIONS

Results of this study revealed contrasted responses of the photosynthetic apparatus in three grassland species under combined environmental stresses in summer. Because stress drivers are multiple and untangled, it is probable that the observed photosynthetic response for the different species results from the combination of different events such as energy dissipation within the antenna, dissociation of LHCII from the PSII supercomplexes, PSII RC silencing, regulation of the electron flow and change in PSI efficiency. The causes for the contrasted responses observed among measured species are yet to be identified and might also depend on plant/leaf anatomy as well as physiological factors such as the phloem loading capacity (Demmig-Adams and Adams, 2006). In a grassland study, Gielen et al. (2007) also suggested that difference in plants height among species might lead to difference in shading and, therefore, different susceptibility to midday photoinhibition between species. Results also highlighted that a decrease in the ecosystem photosynthetic performance did not result in reduced carbon fixation. We wonder if an increase in abundance of the studied dicot species might improve carbon fixation during stress episodes, as the two dicots expressed an enhanced capacity to stimulate PSI efficiency under stressful conditions. However, this response which was associated with improved efficiency in electron transport, might also indicate increased alternative electron sinks, such as photorespiration and/or cyclic electron flow. Further studies are needed to partition the relative contribution of these different electron sinks to PSI activity under stressful conditions. Better understanding of these mechanisms in response to environmental constraints and their impact on ecosystem CO_2 fluxes might be useful in elucidating ecosystem response to climate change and might help in selecting cultivated varieties favoring carbon fixation during stress episodes.

AUTHOR CONTRIBUTIONS

BH, MA, PD, PdJ, CA, NS, and M-LF: planned and designed the research; AD, LdlM, AB, CA, NS, and AM: performed experiments and conducted fieldwork; AD, LdlM, AB, FB, and A-CD: analyzed and interpreted the data; AD: wrote the paper; BH, MA, PD, PdJ, CA, NS, AB, FB, and M-LF: revised the paper.

FUNDING

This work was supported by the National Fund for Scientific Research of Belgium (PDR, no. 14614874).

ACKNOWLEDGMENTS

We are very grateful to A. Genette and E. Hanon for their useful advice and constructive remarks. We also thank M. Eyletters for constructive discussions. We also wish to thank H. Chopin, A. Debacq, and F. Wilmus for their technical support.

SUPPLEMENTARY MATERIAL

The Supplementary Material for this article can be found online at: https://www.frontiersin.org/articles/10.3389/fpls.2018.00067/full#supplementary-material

REFERENCES

Adams, W. W., and Demmig-Adams, B. (2004). "Chlorophyll fluorescence as a tool to monitor plant response to the environment in Papageorgiou," in *Chlorophyll Chlorophyll Fluorescence: A Signature of Photosynthesis,* ed G. C. Govindjee (Dordrecht: Springer), 583–604.

Asada, K. (2006). Production and scavenging of reactive oxygen species in chloroplasts and their functions. *Plant Physiol.* 141, 391–396. doi: 10.1104/pp.106.082040

Ashraf, M., and Harris, P. J. C. (2013). Photosynthesis under stressful environments: an overview. *Photosynthetica* 51, 163–190. doi: 10.1007/s11099-013-0021-6

Atkin, O. K., and Tjoelker, M. G. (2003). Thermal acclimation and the dynamic response of plant respiration to temperature. *Trends Plant Sci.* 8, 343–351. doi: 10.1016/S1360-1385(03)00136-5

Atkin, O. K., Westbeek, M. H. M., Cambridge, M. L., Lambers, H., and Pons, T. L. (1997). Leaf respiration in light and darkness. A comparison of slow- and fast-growing Poa species. *Plant Physiol.* 113, 961–965.

Bai, J., Xu, D. H., Kang, H. M., Chen, K., and Wang, G. (2008). Photoprotective function of photorespiration in *Reaumuria soongorica* during different levels of drought stress in natural high irradiance. *Photosynthetica* 46, 232–237. doi: 10.1007/s11099-008-0037-5

Bertolde, F. Z., Almeida, A.-A. F., Pirovani, C. P., Gomes, F. P., Ahnert, D., Baligar, V. C., et al. (2012). Physiological and biochemical responses of *Theobroma cacao* L. genotypes to flooding. *Photosynthetica* 50, 447–457. doi: 10.1007/s11099-012-0052-4

Bielczynski, L. W., Schansker, G., and Croce, R. (2016). Effect of light acclimation on the organization of photosystem ii super- and sub-complexes in *Arabidopsis thaliana*. *Front. Plant Sci.* 7:105. doi: 10.3389/fpls.2016.00105

Bollig, C., and Feller, U. (2014). Impacts of drought stress on water relations and carbon assimilation in grassland species at different altitudes. *Agric. Ecosyst. Environ.* 188, 212–220. doi: 10.1016/j.agee.2014.02.034

Borchard, N., Schirrmann, M., von Hebel, C., Schmidt, M., Baatz, R., Firbank, L., et al. (2015). Spatio-temporal drivers of soil and ecosystem carbon fluxes at field scale in an upland grassland in Germany. *Agric. Ecosyst. Environ.* 211, 84–93. doi: 10.1016/j.agee.2015.05.008

Boughalleb, F., Denden, M., and Ben Tiba, B. (2009). Photosystem II photochemistry and physiological parameters of three fodder shrubs, *Nitraria retusa*, *Atriplex halimus* and *Medicago arborea* under salt stress. *Acta Physiol. Plant.* 31, 463–476. doi: 10.1007/s11738-008-0254-3

Brestic, M., Zivcak, M., Kalaji, H. M., Carpentier, R., and Allakhverdiev, S. I. (2012). Photosystem II thermostability *in situ*: environmentally induced acclimation and genotype-specific reactions in *Triticum aestivum* L. *Plant Physiol. Biochem.* 57, 93–105. doi: 10.1016/j.plaphy.2012.05.012

Bussotti, F. (2004). Assessment of stress conditions in *Quercus ilex* L. leaves by O-J-I-P chlorophyll a fluorescence analysis. *Plant Biosystem.* 138, 101–109. doi: 10.1080/11263500412331283708

Bussotti, F., Desotgiu, R., Cascio, C., Pollastrini, M., Gravano, E., Gerosa, G., et al. (2011). Ozone stress in woody plants assessed with chlorophyll a fluorescence. A critical reassessment of existing data. *Environ. Exp. Bot.* 73, 19–30. doi: 10.1016/j.envexpbot.2010.10.022

Bussotti, F., Desotgiu, R., Pollastrini, M., and Cascio, C. (2010). The JIP test: a tool to screen the capacity of plant adaptation to climate change. *Scand. J. Forest Res.* 25, 43–50. doi: 10.1080/02827581.2010.485777

Bussotti, F., Strasser, R. J., and Schaub, M. (2007). Photosynthetic behavior of woody species under high ozone exposure probed with the JIP-test: a review. *Environ. Pollut.* 147, 430–437. doi: 10.1016/j.envpol.2006.08.036

Campos, H., Trejo, C., Peña-Valdivia, C. B., García-Nava, R., Conde-Martínez, F. V., and Cruz-Ortega, M. D. R. (2014). Photosynthetic acclimation to drought stress in *Agave salmiana* Otto ex Salm-Dyck seedlings is largely dependent on thermal dissipation and enhanced electron flux to photosystem I. *Photosynth. Res.* 122, 23–39. doi: 10.1007/s11120-014-0008-6

Cascio, C., Schaub, M., Novak, K., Desotgiu, R., Bussotti, F., and Strasser, R. J. (2010). Foliar responses to ozone of *Fagus sylvatica* L. seedlings grown in shaded and in full sunlight conditions. *Environ. Exp. Bot.* 68, 188–197. doi: 10.1016/j.envexpbot.2009.10.003

Chen, J., Luo, Y., Xia, J., Wilcox, K. R., Cao, J., Zhou, X., et al. (2017). Warming effects on ecosystem carbon fluxes are modulated by plant functional types. *Ecosystems* 20:515. doi: 10.1007/s10021-016-0035-6

Chen, J., Zhou, X., Wang, J., Hruska, T., Shi, W., Cao, J., et al. (2016). Grazing exclusion reduced soil respiration but increased its temperature sensitivity in a meadow grassland on the Tibetan plateau. *Ecol. Evol.* 6, 675–687. doi: 10.1002/ece3.1867

Ciccarelli, D., Picciarelli, P., Bedini, G., and Sorce, C. (2016). Mediterranean sea cliff plants: morphological and physiological responses to environmental conditions. *J. Plant Ecol.* 9, 153–164. doi: 10.1093/jpe/rtv042

Dagnelie, P. (2013). *Statistique Théorique et Appliquée, Tome 1, Statistique Descriptive et Bases de L'inférence Statistique*. Bruxelles: de Boeck.

Demmig-Adams, B., and Adams, W. W. (2006). Photoprotection in an ecological context: the remarkable complexity of thermal energy dissipation. *New Phytol.* 172, 11–21. doi: 10.1111/j.1469-8137.2006.01835.x

Derks, A., Schaven, K., and Bruce, D. (2015). Diverse mechanisms for photoprotection in photosynthesis. Dynamic regulation of photosystem II excitation in response to rapid environmental change. *Biochim. Biophys. Acta* 1847, 468–485. doi: 10.1016/j.bbabio.2015.02.008

Desotgiu, R., Cascio, C., Pollastrini, M., Gerosa, G., Marzuoli, R., and Bussotti, F. (2012a). Short and long term photosynthetic adjustments in sun and shade leaves of *Fagus sylvatica* L., investigated by fluorescence transient (FT) analysis. *Plant Biosyst.* 146, 206–216. doi: 10.1080/11263504.2012.705350

Desotgiu, R., Pollastrini, M., Cascio, C., Gerosa, G., Marzuoli, R., and Bussotti, F. (2012b). Chlorophyll alpha fluorescence analysis along a vertical gradient of the crown in a poplar (Oxford clone) subjected to ozone and water stress. *Tree Physiol.* 32, 976–986. doi: 10.1093/treephys/tps062

Digrado, A., Bachy, A., Mozaffar, A., Schoon, N., Dalcq, A.-C., Amelynck, C., et al. (2017). Long-term measurements of chlorophyll a fluorescence using the JIP-test show that combined abiotic stresses influence the photosynthetic performance of the perennial ryegrass (*Lolium perenne* L.) in a managed temperate grassland. *Physiol. Plant.* 161, 355–371. doi: 10.1111/ppl.12594

Feller, U. (2016). Drought stress and carbon assimilation in a warming climate: reversible and irreversible impacts. *J. Plant Physiol.* 203, 84–94. doi: 10.1016/j.jplph.2016.04.002

Fernández-Baco, L., Figueroa, M. E., Luque, T., and Davy, A. J. (1998). Diurnal and seasonal variations in chlorophyll a fluorescence in two mediterranean-grassland species under field conditions. *Photosynthetica* 35, 535–544. doi: 10.1023/A:1006926923293

Fox, J., Weisberg, S., Adler, D., Bates, D., Baud-Bovy, G., Ellison, S., et al. (2016). *Car: Companion to Applied Regression.* Available online at: http://www.R-project.org/ (accessed March 16, 2017).

Ganjurjav, H., Gao, Q., Borjigidai, A., Guo, Y., Wan, Y., Li, Y., et al. (2014). Alpine grassland ecosystem respiration variation under irrigation in Northern Tibet. *Acta Ecol. Sin.* 34, 271–276. doi: 10.1016/j.chnaes.2014.07.004

Ghotbi-Ravandi, A. A., Shahbazi, M., Shariati, M., and Mulo, P. (2014). Effects of mild and severe drought stress on photosynthetic efficiency in tolerant and susceptible barley (*Hordeum vulgare* L.) genotypes. *J. Agron. Crop Sci.* 200, 403–415. doi: 10.1111/jac.12062

Gielen, B., Naudts, K., D'Haese, D., Lemmens, C. M., De Boeck, H. J., Biebaut, E., et al. (2007). Effects of climate warming and species richness on photochemistry of grasslands. *Physiol. Plant.* 131, 251–262. doi: 10.1111/j.1399-3054.2007.00951.x

Goh, C.-H., Ko, S.-M., Koh, S., Kim, Y.-J., and Bae, H.-J. (2012). Photosynthesis and environments: photoinhibition and repair mechanisms in plants. *J. Plant Biol.* 55, 93–101. doi: 10.1007/s12374-011-9195-2

Goltsev, V., Zaharieva, I., Chernev, P., Kouzmanova, M., Kalaji, H. M., Yordanov, I., et al. (2012). Drought-induced modifications of photosynthetic electron transport in intact leaves: analysis and use of neural networks as a tool for a rapid non-invasive estimation. *Biochim. Biophys. Acta* 1817, 1490–1498. doi: 10.1016/j.bbabio.2012.04.018

Gourlez de la Motte, L., Jérôme, E., Mamadou, O., Beckers, Y., Bodson, B., Heinesch, B., et al. (2016). Carbon balance of an intensively grazed permanent grassland in southern Belgium. *Agricult. Forest Meteorol.* 228, 370–383. doi: 10.1016/j.agrformet.2016.06.009

Gravano, E., Bussotti, F., Strasser, R. J., Schaub, M., Novak, K., Skelly, J., et al. (2004). Ozone symptoms in leaves of woody plants in open-top chambers:

ultrastructural and physiological characteristics. *Physiol. Plant.* 121, 620–633. doi: 10.1111/j.1399-3054.2004.00363.x

Groemping, U., and Matthias, L. (2013). *Relaimpo: Relative Importance of Regressors in Linear Models.* Available online at http://www.R-project.org/ (Accessed March 16, 2017)

Guidi, L., and Calatayud, A. (2014). Non-invasive tools to estimate stress-induced changes in photosynthetic performance in plants inhabiting Mediterranean areas. *Environ. Exp. Bot.* 103, 42–52. doi: 10.1016/j.envexpbot.2013.12.007

Heskel, M. A., Atkin, O. K., Turnbull, M. H., and Griffin, K. L. (2013). Bringing the Kok effect to light: a review on the integration of daytime respiration and net ecosystem exchange. *Ecosphere* 4, 1–14. doi: 10.1890/ES13-00120.1

Hill, P. W., Garnett, M. H., Farrar, J., Iqbal, Z., Khalid, M., Soleman, N., et al. (2015). Living roots magnify the response of soil organic carbon decomposition to temperature in temperate grassland. *Glob. Chang. Biol.* 21, 1368–1375. doi: 10.1111/gcb.12784

Hoover, D. L., Knapp, A. K., and Smith, M. D. (2016). The immediate and prolonged effects of climate extremes on soil respiration in a mesic grassland. *J. Geophys. Res. Biogeosci.* 121, 1034–1044. doi: 10.1002/2015JG003256

Husson, F., Josse, J., Le, S., and Mazet, J. (2016). *FactoMineR: Multivariate Exploratory Data Analysis and Data Mining*. Available online at http://www.R-project.org/ (Accessed March 16, 2017).

Jahns, P., and Holzwarth, A. R. (2012). The role of the xanthophyll cycle and of lutein in photoprotection of photosystem II. *Biochim. Biophys. Acta* 1817, 182–193. doi: 10.1016/j.bbabio.2011.04.012

Janka, E., Körner, O., Rosenqvist, E., and Ottosen, C.-O. (2013). High temperature stress monitoring and detection using chlorophyll a fluorescence and infrared thermography in chrysanthemum (*Dendranthema grandiflora*). *Plant Physiol. Biochem.* 67, 87–94. doi: 10.1016/j.plaphy.2013.02.025

Jedmowski, C., Bayramov, S., and Brüggemann, W. (2014). Comparative analysis of drought stress effects on photosynthesis of Eurasian and North African genotypes of wild barley. *Photosynthetica* 52, 564–573. doi: 10.1007/s11099-014-0064-3

Kalaji, H. M., Carpentier, R., Allakhverdiev, S. I., and Bosa, K. (2012). Fluorescence parameters as early indicators of light stress in barley. *J. Photochem. Photobiol. Biol.* 112, 1–6. doi: 10.1016/j.jphotobiol.2012.03.009

Kalaji, H. M., Jajoo, A., Oukarroum, A., Brestic, M., Zivcak, M., Samborska, I. A., et al. (2016). Chlorophyll a fluorescence as a tool to monitor physiological status of plants under abiotic stress conditions. *Acta Physiol. Plant.* 38:102. doi: 10.1007/s11738-016-2113-y

Kalaji, H. M., Schansker, G., Brestic, M., Bussotti, F., Calatayud, A., Ferroni, L., et al. (2017). Frequently asked questions about chlorophyll fluorescence, the sequel. *Photosyn. Res.* 132, 13–66. doi: 10.1007/s11120-016-0318-y

Kataria, S., and Guruprasad, K. N. (2015). Exclusion of solar UV radiation frequently asked questions about chlorophyll fluorescence, the sequel improves photosynthetic performance and yield of wheat varieties. *Plant Physiol. Biochem.* 97, 400–411. doi: 10.1016/j.plaphy.2015.10.001

Lee, H.-Y., Chow, W. S., and Hong, Y.-N. (1999). Photoinactivation of photosystem II in leaves of *Capsicum annuum*. *Physiol. Plant.* 105, 376–383. doi: 10.1034/j.1399-3054.1999.105224.x

Lloyd, J., and Taylor, J. A. (1994). On the temperature dependence of soil respiration. *Funct. Ecol.* 8, 315–323. doi: 10.2307/2389824

Mamadou, O., Gourlez de la Motte, L., De Ligne, A., Heinesch, B., and Aubinet, M. (2016). Sensitivity of the annual net ecosystem exchange to the cospectral model used for high frequency loss corrections at a grazed grassland site. *Agricult. Forest Meteorol.* 228–229, 360–369. doi: 10.1016/j.agrformet.2016.06.008

Massacci, A., Nabiev, S. M., Pietrosanti, L., Nematov, S. K., Chernikova, T. N., Thor, K., et al. (2008). Response of the photosynthetic apparatus of cotton (*Gossypium hirsutum*) to the onset of drought stress under field conditions studied by gas-exchange analysis and chlorophyll fluorescence imaging. *Plant Physiol. Biochem.* 46, 189–195. doi: 10.1016/j.plaphy.2007.10.006

Mathur, S., and Jajoo, A. (2015). Investigating deleterious effects of ultraviolet (UV) radiations on wheat by a quick method. *Acta Physiol. Plant.* 37:121. doi: 10.1007/s11738-015-1874-z

Mathur, S., Jajoo, A., Mehta, P., and Bharti, S. (2011). Analysis of elevated temperature-induced inhibition of photosystem II using chlorophyll a fluorescence induction kinetics in wheat leaves (*Triticum aestivum*). *Plant Biol.* 13, 1–6. doi: 10.1111/j.1438-8677.2009.00319.x

Maxwell, K., and Johnson, G. N. (2000). Chlorophyll fluorescence - a practical guide. *J. Exp. Bot.* 51, 659–668. doi: 10.1093/jexbot/51.345.659

Menzel, U. (2015). *CCP: Significance Tests for Canonical Correlation Analysis (CCA).* Available online at: http://www.R-project.org/ (accessed March 16, 2017).

Murchie, E. H., and Lawson, T. (2013). Chlorophyll fluorescence analysis: a guide to good practice and understanding some new applications. *J. Exp. Bot.* 64, 3983–3998. doi: 10.1093/jxb/ert208

Oksanen, J., Blanchet, F. G., Friendly, M., Kindt, R., Legendre, P., McGlinn, D., et al. (2012). *Vegan : Community Ecology Package.* Available online at http://www.R-project.org/ (accessed March 16, 2017).

Osório, M. L., Osório, J., and Romano, A. (2013). Photosynthesis, energy partitioning, and metabolic adjustments of the endangered Cistaceae species Tuberaria major under high temperature and drought. *Photosynthetica* 51, 75–84. doi: 10.1007/s11099-012-0080-0

Oukarroum, A., El Madidi, S., and Strasser, R. J. (2016). Differential heat sensitivity index in barley cultivars (*Hordeum vulgare* L.) monitored by chlorophyll a fluorescence OKJIP. *Plant Physiol. Biochem.* 105, 102–108. doi: 10.1016/j.plaphy.2016.04.015

Pettigrew, W. T. (2016). Cultivar variation in cotton photosynthetic performance under different temperature regimes. *Photosynthetica* 54, 502–507. doi: 10.1007/s11099-016-0208-8

Pollastrini, M., Di Stefano, V., Ferretti, M., Agati, G., Grifoni, D., Zipoli, G., et al. (2011). Influence of different light intensity regimes on leaf features of *Vitis vinifera* L. in ultraviolet radiation filtered condition. *Environ. Exp. Bot.* 73, 108–115. doi: 10.1016/j.envexpbot.2010.10.027

Pollastrini, M., Holland, V., Brüggemann, W., Bruelheide, H., Dănilă, I., Jaroszewicz, B., et al. (2016a). Taxonomic and ecological relevance of the chlorophyll a fluorescence signature of tree species in mixed European forests. *New Phytol.* 212, 51–65. doi: 10.1111/nph.14026

Pollastrini, M., Holland, V., Brüggemann, W., and Bussotti, F. (2016b). Chlorophyll a fluorescence analysis in forests. *Annal. Bot.* 6, 23–37. doi: 10.4462/annbotrm-13257

R Development Core Team. (2012). *R: A Language and Environment for Statistical Computing.* Vienna, Austria: R Foundation for Statistical Computing. Available online at http://www.R-project.org/ (accessed March 16, 2017).

Redillas, M. C. F. R., Strasser, R. J., Jeong, J. S., Kim, Y. S., and Kim, J.-K. (2011). The use of JIP test to evaluate drought-tolerance of transgenic rice overexpressing OsNAC10. *Plant Biotechnol. Rep.* 5, 169–175. doi: 10.1007/s11816-011-0170-7

Reichstein, M., Falge, E., Baldocchi, D., Papale, D., Aubinet, M., Berbigier, P., et al. (2005). On the separation of net ecosystem exchange into assimilation and ecosystem respiration: review and improved algorithm. *Glob. Chang. Biol.* 11, 1424–1439. doi: 10.1111/j.1365-2486.2005.001002.x

Rho, H., Yu, D. J., Kim, S. J., and Lee, H. J. (2012). Limitation factors for photosynthesis in 'Bluecrop' highbush blueberry (*Vaccinium corymbosum*) leaves in response to moderate water stress. *J. Plant Biol.* 55, 450–457. doi: 10.1007/s12374-012-0261-1

Sage, R. F. (2013). Photorespiratory compensation: a driver for biological diversity. *Plant Biol.* 15, 624–638. doi: 10.1111/plb.12024

Scheller, H. V., and Haldrup, A. (2005). Photoinhibition of photosystem I. *Planta* 221, 5–8. doi: 10.1007/s00425-005-1507-7

Smit, M. F., Kruger, G. H. J., van Heerden, P. D. R., Pienaar, J. J., Weissflog, L., and Strasser, R. J. (2009). "Effect of trifluoroacetate, a persistent degradation product of fluorinated hydrocarbons, on C3 and C4 crop plants," in *Photosynthesis. Energy from the sun. 14th International Congress of Photosynthesis Glasgow 2007,* eds J. F Allen, E. Gantt, J. H. Golbeck, B. Osmond (Dordrecht: Springer), 623–634.

Strasser, R., Srivastava, A., and Tsimilli-Michael, M. (2000). "The fluorescence transient as a tool to characterize and screen photosynthetic samples," in *Probing Photosynthesis: Mechanism, Regulation and Adaptation,* eds M. Yunnus, U. Pathre, and P. Mohanty (London: Taylor and Francis), 443–480.

Strasser, R., Tsimilli-Michael, M., and Srivastava, A. (2004). "Analysis of the chlorophyll a transient," in *Chlorophyll Chlorophyll Fluorescence: A Signature of Photosynthesis,* eds Govindjee, G. C. Papageorgiou (Dordrecht: Springer), 321–362.

Stroch, M., Vrábl, D., Podolinská, J., and Kalina, J., Urban, O., and Spunda, V. (2010). Acclimation of Norway spruce photosynthetic apparatus to the combined effect of high irradiance and temperature. *J. Plant Physiol.* 167, 597–605. doi: 10.1016/j.jplph.2009.11.011

Takahashi, S., Milward, S. E., Fan, D.-Y., Chow, W. S., and Badger, M. R. (2009). How does cyclic electron flow alleviate photoinhibition in Arabidopsis? *Plant Physiol.* 149, 1560–1567. doi: 10.1104/pp.108.134122

Tiwari, A., Mamedov, F., Grieco, M., Suorsa, M., Jajoo, A., Styring, S., et al. (2016). Photodamage of iron–sulphur clusters in photosystem I induces non-photochemical energy dissipation. *Nat. Plants* 2:16035. doi: 10.1038/nplants.2016.35

Tozzi, E. S., Easlon, H. M., and Richards, J. H. (2013). Interactive effects of water, light and heat stress on photosynthesis in Fremont cottonwood. *Plant Cell Environ.* 36, 1423–1434. doi: 10.1111/pce.12070

Tsimilli-Michael, M., and Strasser, R. J. (2008). "*In vivo* assessment of stress impact on plant's vitality: applications in detecting and evaluating the beneficial role of mycorrhization on host plants," in *Mycorrhiza: State of the Art, Genetics and Molecular Biology, Eco-Function, Biotechnology, Eco- Physiology, Structure and Systematics*, *Vol. 3,* ed A. Varma (Dordrecht: Springer), 679–703.

van Heerden, P. D. R., Tsimilli-Michael, M., Krüger, G. H. J., Strasser, R. J., and Kruger, G. H. J. (2003). Dark chilling effects on soybean genotypes during vegetative development: parallel studies of CO_2 assimilation, chlorophyll a fluorescence kinetics O-J-I-P and nitrogen fixation. *Physiol. Plant.* 117, 476–491. doi: 10.1034/j.1399-3054.2003.00056.x

Voss, I., Sunil, B., Scheibe, R., and Raghavendra, A. S. (2013). Emerging concept for the role of photorespiration as an important part of abiotic stress response. *Plant Biol.* 15, 713–722. doi: 10.1111/j.1438-8677.2012.00710.x

Wehr, R., Munger, J. W., McManus, J. B., Nelson, D. D., Zahniser, M. S., Davidson, E. A., et al. (2016). Seasonality of temperate forest photosynthesis and daytime respiration. *Nature* 534, 680–683. doi: 10.1038/nature17966

Werner, C., Correia, O., and Beyschlag, W. (2002). Characteristic patterns of chronic and dynamic photoinhibition of different functional groups in a Mediterranean ecosystem. *Funct. Plant Biol.* 29, 999–1011. doi: 10.1071/PP01143

Werner, C., Ryel, R. J., Correia, O., and Beyschlag, W. (2001). Effects of photoinhibition on whole-plant carbon gain assessed with a photosynthesis model. *Plant Cell Environ.* 24, 27–40. doi: 10.1046/j.1365-3040.2001.00651.x

Wohlfahrt, G., and Gu, L. (2015). The many meanings of gross photosynthesis and their implication for photosynthesis research from leaf to globe. *Plant Cell Environ.* 38, 2500–2507. doi: 10.1111/pce.12569

Xu, Z. Z., Zhou, G. S., Wang, Y. L., Han, G. X., and Li, Y. J. (2008). Changes in chlorophyll fluorescence in maize plants with imposed rapid dehydration at different leaf ages. *J. Plant Growth Regul.* 27, 83–92. doi: 10.1007/s00344-007-9035-2

Zhu, L., Johnson, D. A., Wang, W., Ma, L., and Rong, Y. (2015). Grazing effects on carbon fluxes in a Northern China grassland. *J. Arid Environ.* 114, 41–48. doi: 10.1016/j.jaridenv.2014.11.004

Conflict of Interest Statement: The authors declare that the research was conducted in the absence of any commercial or financial relationships that could be construed as a potential conflict of interest.

The reviewer LF declared a past co-authorship with one of the authors FB to the handling Editor, who ensured that the process met the standards of a fair and objective review.